PERGAMON

International Journal of Heat and Mass Transfer 44 (2001) 1143–1151

International Journal of HEAT and MASS TRANSFER

www.elsevier.com/locate/ijhmt

Natural convection heat and mass transfer in vertical annuli with film evaporation and condensation

Wei-Mon Yan *, David Lin

Department of Mechanical Engineering, Huafan University, Shih-Ting, Taipei 22305, Taiwan, ROC

Received 26 April 1999; received in revised form 5 May 2000

Abstract

A numerical study of natural convection heat and mass transfer with film evaporation and condensation in vertical concentric annular ducts is performed. The emphasis is focused on the effects of the film evaporation and condensation along the wetted walls on the heat and mass transfer in vertical annuli. The numerical results, including the velocity, temperature and concentration profiles, local Nusselt and Sherwood numbers and induced volume flow rate are presented for air–water vapor system under different wall temperature T_1 and ratio of radii λ. The results show that tremendous enhancement in heat transfer due to the exchange of latent heat in association with film evaporation and condensation was found. In addition, the extent of augmentation of heat transfer due to mass transfer is more significant for a system with a higher wetted wall temperature T_1.

1. Introduction

There are many physical processes in which buoyancy forces from thermal diffusion and diffusion of chemical species simultaneously play an important role in the transfer of heat and mass. Noticeable examples include the chemical distillatory processes, design of heat exchangers, channel type solar energy collectors, and thermo-protection systems. Hence, the characteristics of natural convection heat and mass transfer are relatively important.

The natural convection heat transfer in vertical open annular duct flows induced by the thermal buoyancy force alone has been investigated in great detail in literature [1–5]. The effects of mass diffusion on natural convection flows along flat plate with different inclination have been studied rather extensively [6–10]. In contrast to external natural convection heat and mass transfer, the natural convection heat and mass transfer in internal flows has been examined for vertical parallel plates [11–14] and for vertical tube [15]. Regardless of its importance in engineering applications, the natural convection heat and mass transfer in vertical open annular ducts has not been well evaluated. This motivates the present investigation.

The geometry of the present problem under consideration is a vertical annulus of finite length l open at both ends (see Fig. 1). The inner and outer radii are R_1 and R_2, respectively. Both the inner and outer walls are wetted by thin liquid water films. The inner and outer walls are, respectively, maintained at uniform but different temperature levels, T_1 and T_2, higher than the ambient temperature T_0. The flow of moist air is drawn into the annular gap between the two cylindrical walls by natural convection induced by the non-uniformities in temperature and in concentration of water vapor in the flow. Attention is focused on the study of the latent heat transport in conjunction with the evaporation or condensation of water vapor along the wetted walls.

2. Analysis

To facilitate the analysis, the liquid film on the wetted walls are assumed to be extremely thin so that they can be treated with boundary conditions. In reality, the

* Corresponding author. Tel.: +886-2-2663-2102 ext. 4038; fax: +886-2-2663-3847.

E-mail addresses: wmyan@huafan.hfu.edu.tw (W.-M. Yan), david@huafan.hfu.edu.tw (D. Lin).

0017-9310/01/$ - see front matter
PII: S0017-9310(00)00176-9

Nomenclature

A	$[(c_{pv}-c_{pa})/c_p]\ (w_1-w_0)$
c_p	specific heat
D	mass diffusivity
D_h	equivalent hydraulic diameter, $2(R_2-R_1)$
Gr_M	Grashof number (mass transfer), $g(M_a/M_v-1)(w_1-w_0)D_h^4/(lv^2)$
Gr_T	Grashof number (heat transfer), $g\beta(T_1-T_0)\ D_h^4/(lv^2)$
g	gravitational acceleration
h	heat transfer coefficient
h_{fg}	latent heat of vaporization or condensation
k	thermal conductivity
L	dimensionless channel length, $1/Gr_r$
M	molecular weight
Nu_l	local Nusselt number (latent heat)
Nu_s	local Nusselt number (sensible heat)
Nu_x	local Nusselt number $(=Nu_s+Nu_l)$
P	dimensionless dynamic pressure
p_1, p_2	partial pressures on the inner and outer walls, respectively
Pr	Prandtl number, v/α
r	radial number
R_1, R_2	inner and outer radii, respectively
Re	Reynolds number at inlet
S	parameter, Eq. (15)
Sc	Schmidt number, v/D
Sh	Sherwood number
T	temperature
T_1	inner wall temperature
T_2	outer wall temperature
T_0	inlet temperature
u_0, U_0	dimensional and dimensionless induced axial velocity at inlet
U, V	dimensionless velocity components in the x and r directions, respectively
V_1, V_2	dimensionless interfacial velocities of mixture along the wetted walls
w, W	dimensional and dimensionless species concentration, respectively
Y	dimensionless radial coordinate, $Y=(r-R_1)/(R_2-R_1)$

Greek symbols

α	thermal diffusivity
β	coefficient of thermal expansion
β^*	coefficient of concentration expansion
η	dimensionless radial coordinate, r/R_2
θ	$(T-T_0)/(T_1-T_0)$
λ	radius ratio, R_1/R_2
v	kinematic viscosity
ξ	dimensionless axial coordinate, $x/(lGr_r)$
ρ	density
l	channel height
ϕ	relative humidity of moist in the ambient

Subscripts

a	of air
0	value at inlet
r	at reference condition
v	of water vapor
1	condition at inner wall; i.e., at $r=R_1$
2	condition at outer wall; i.e., at $r=R_2$

liquid films on the wetted walls are of finite thickness. They would move due to gravity effect and interact with the induced gas flow. However, this would complicate the present problem. In the related study of the present author, it was found that the assumption of extremely thin film thickness is reasonable as the film thickness is relatively thin [14]. In addition, an order of magnitude analysis is employed, which deduces the governing equations by neglecting the axial diffusion of momentum, heat and mass. The thermophysical properties of the mixture are taken to be constant and calculated by the one-third rule [16]. The complete details on the evaluation of the properties of air, water vapor and their mixture are available in Refs. [17,18]. Although the mixture has constant thermophysical properties but obeys the Boussinesq approximation, according to which its density is constant except in the buoyancy term of the axial momentum equation. With the above assumptions, the steady natural convection heat and mass transfer in vertical annuli can be described by the following dimensionless governing equations.

Continuity equation:

$$\partial(\eta U)/\partial\xi+\partial(\eta V)/\partial\eta=0. \tag{1}$$

Axial-momentum equation:

$$\begin{aligned}U\partial U/\partial\xi+V\partial U/\partial\eta&=-\mathrm{d}P/\mathrm{d}\xi+1/\eta\cdot\partial(\eta\partial U/\partial\eta)/\partial\eta\\&\quad+(Gr_T\theta+Gr_M W)/[16(Gr_{Tr}+Gr_{Mr})\cdot(1-\lambda)^4].\end{aligned} \tag{2}$$

Energy equation:

$$\begin{aligned}U\partial\theta/\partial\xi+V\partial\theta/\partial\eta&=1/(Pr\cdot\eta)\cdot\partial(\eta\partial\theta/\partial\eta)\\&\quad+A/Sc\cdot(\partial\theta/\partial\eta)\cdot(\partial W/\partial\eta).\end{aligned} \tag{3}$$

Concentration equation of water vapor:

$$U\partial W/\partial\xi+V\partial W/\partial\eta=1/(Sc\cdot\eta)\cdot\partial(\eta\partial W/\partial\eta)/\partial\eta. \tag{4}$$

In non-dimensionalizing the governing equations, the following dimensionless variables were introduced

$$\xi = x/(lGr_r),\ \ \eta = r/R_2,$$
$$Y = (\eta-\lambda)/(1-\lambda),\ \ U = uR_2^2/(lvGr_r),$$
$$V = vR_2/v,\ \ \theta = (T-T_0)/(T_1-T_0),$$
$$W = (w-w_0)/(w_1-w_0),\ \ r_T = (T_2-T_0)/(T_1-T_0),$$
$$r_w = (w_2-w_0)/(w_1-w_0),\ \ P = p_m R_2^4/\left(\rho l^2 v^2 Gr_r^2\right),$$
$$\lambda = R_1/R_2,\ \ Gr_T = g(T_1-T_0)D_h^4/(lv^2T_0),$$
$$Gr_M = g(M_a/M_v-1)(w_1-w_0)D_h^4/(lv^2),\ \ D_h = 2(1-\lambda)R_2,$$
$$A = \left[\left(c_{pv}-c_{pa}\right)/c_p\right](w_1-w_0),\ \ Gr_r = Gr_{Tr}+Gr_{Mr}. \tag{5}$$

It is worth noting that Gr_{Tr} and Gr_{Mr} are, respectively, the Grashof numbers for heat and mass transfer at the reference condition, as shown in the last row of Table 1. The use of Gr_{Tr} and Gr_{Mr} leads to a physically more meaningful comparison among various case studies.

The dimensionless boundary conditions of this problem are

$$\xi = 0 : U = U_0, \quad \theta = 0, \quad W = 0, \quad P = -U_0^2/2, \tag{6a}$$

$$\eta = \lambda : U = 0, \quad V = V_1(\xi), \quad \theta = 1, \quad W = 1, \tag{6b}$$

$$\eta = 1 : U = 0, \quad V = V_2(\xi), \quad \theta = r_T, \quad W = r_W, \tag{6c}$$

$$\xi = L = 1/(Gr_{Tr}+Gr_{Mr}) : P = 0. \tag{6d}$$

Notice that air–water interfaces are semipermeable, that is, the solubility of air in water is negligibly small and air is stationary at the interfaces, the radial velocities on the inner and outer wetted walls can be evaluated by [19]

$$V_i = -(w_1-w_0)/(1-w_i)\cdot(\partial W/\partial\eta)/Sc, \quad i = 1,2. \tag{7}$$

According to Daltons' law and the state equation of ideal gas mixture, the interfacial mass-fraction of water vapor can be calculated by [18]

$$w_i = p_i M_V/[p_i M_V + (p-p_i)M_a], \quad i = 1,2, \tag{8}$$

where p_i is the saturated water vapor pressure on the wetted walls. It should be mentioned here that the pressure defects at the inlet and exit are determined by the equations $P = -U_0^2/2$ and $P = 0$, respectively. Strictly speaking, pressure conditions at the inlet and exit should be evaluated by a more complete analysis including not only the flow in the channel but also the flows in the immediate surroundings around the inlet and exit. This would greatly complicate the analysis and is beyond the scope of the present work. But it is noticed that as far as the heat and mass transfer characteristics are concerned, the boundary-layer type of analysis performed here is good in practical applications [11]. For a specific geometry of the concentric annulus and heating condition, there exits an inlet velocity U_0 which yields $P = 0$ at the exit of the annulus. In the present study, U_0 was obtained in the solution process iteratively.

One constraint to be satisfied in the study of the steady channel flow is the overall mass balance at every axial location

$$\int_\lambda^1 \eta U\,\mathrm{d}\eta = U_0\cdot\left(1-\lambda^2\right)/2 + \int_0^\xi (\lambda V_1 - V_2)\,\mathrm{d}\xi. \tag{9}$$

The above equation is used in the solution process to deduce the pressure gradient in the flow.

The local Nusselt and Sherwood numbers are major parameters of interest in the study of convection heat and mass transfer. The total heat flux from the wetted walls can be expressed as

$$q_{x1} = q_{s1} + q_{l1} = -(k\partial T/\partial r)_1 - \left[\rho D h_{fg1}/(1-w_1)\right]\cdot(\partial w/\partial\eta)_1, \tag{10a}$$

$$q_{x2} = q_{s2} + q_{l2} = (k\partial T/\partial r)_2 + \left[\rho D h_{fg2}/(1-w_2)\right]\cdot(\partial w/\partial\eta)_2, \tag{10b}$$

where q_{xi}, q_{si} and q_{li} $(i = 1$ or $2)$ denote the interfacial heat flux, sensible heat flux and latent heat flux, respectively. The local Nusselt numbers along the wetted walls, defined as

$$Nu_{xi} = h_i D_h/k = q_{xi}/[k(T_1-T_0)/D_h], \quad i = 1,2 \tag{11}$$

can be written as

$$Nu_{xi} = Nu_{si} + Nu_{li}, \quad i = 1,2, \tag{12}$$

Table 1
Values of the major parameters

Case	T_1 (°C)	T_2 (°C)	ϕ (%)	λ	l (m)	Gr_T	Gr_M	Pr	Sc
I	30	30	50	0.5	0.5	440.68	151.36	0.706	0.594
II	50	30	50	0.5	0.5	1233.99	529.58	0.706	0.591
III	70	30	50	0.5	0.5	1949.15	1455.62	0.700	0.583
IV	50	30	10	0.5	0.5	1232.64	571.29	0.703	0.591
V	50	30	90	0.5	0.5	1235.34	487.47	0.703	0.591
VI	50	30	50	0.2	0.5	8087.08	3470.63	0.703	0.591
VII	50	30	50	0.8	0.5	31.59	13.56	0.703	0.591
Ref.	50	30	50	0.5	0.5	617.00	264.79	0.703	0.591

where

$$Nu_{s1} = -2(1-\lambda)\cdot(\partial\theta/\partial\eta)_1, \tag{13a}$$

$$Nu_{s2} = 2(1-\lambda)\cdot(\partial\theta/\partial\eta)_2, \tag{13b}$$

$$Nu_{l1} = -[2(1-\lambda)S_1/(1-w_1)]\cdot(\partial W/\partial\eta)_1, \tag{14a}$$

$$Nu_{l2} = [2(1-\lambda)S_2/(1-w_2)]\cdot(\partial W/\partial\eta)_2, \tag{14b}$$

where S_1 and S_2 signify the importance of the energy transport through species diffusion relative to that through thermal diffusion

$$S_i = \rho D h_{fgi}(w_1 - w_0)/[k(T_1 - T_0)], \quad i = 1, 2. \tag{15}$$

Similarly, the local Sherwood numbers can be expressed as

$$Sh_1 = -2(1-\lambda)\cdot(\partial W/\partial\eta)_1, \tag{16a}$$

$$Sh_2 = 2(1-\lambda)\cdot(\partial W/\partial\eta)_2. \tag{16b}$$

3. Solution method

In this work, a marching finite-difference scheme was employed to solve Eqs. (1)–(4) for U, V, θ and W. In the cross-stream direction (η) , 81 non-uniform grid points were used. The grid was uniform in the η direction. Some of the calculations were tested using 161 grid points in the η direction, but no significant improvement over the 81 grid points was found. Additionally, the marching step in the flow direction (ξ) was taken to be $0.001L$ where L is the dimensionless channel length. The subsequential axial step size is enlarged by 3% over the upstream step size. In the program test, a finer axial step size was tried and found to give acceptable accuracy. In writing the finite-difference equations, a fully implicit numerical scheme in which the axial convection is approximated by the upstream difference and the radial convection and diffusion terms by the central difference is employed to transform the governing equations into the finite-difference equations. Each of the finite-difference equations forms a tridiagonal matrix equation, which can be efficiently solved by the Thomas algorithm [20]. To further check the adequacy of the numerical scheme used in the present study, the results for the limiting case of natural convection heat transfer in vertical annuli were first obtained. Excellent agreement between the present predictions and those of El-Shaarawi and Shrhan [1] was found. Through these program tests, it was found that the present numerical method is suitable for this work.

4. Results and discussion

In the present study, calculations are specifically performed for moist air flowing in vertical concentric annuli. Other mixtures can be solved similarly. It should be mentioned that not all the non-dimensional parameters appearing in this work, i.e., Pr, Sc, Gr_T, Gr_M, λ, etc., can be arbitrarily assigned. In fact, they are interdependent for a given mixture under certain specific conditions. In light of the practical situations, T_0, T_1, T_2, ϕ, λ, and l are selected as the independent physical parameters. All the non-dimensional parameters can then be evaluated. Results are obtained for several cases presented in Table 1 (see Fig. 1).

Fig. 2 presents the axial developments of velocity profiles in the duct under various conditions. For comparison's purposes, the results without mass transfer are also plotted in these subplots by the dashed curves. It is clearly seen that the velocity profiles develop gradually from uniform distributions at the inlet to the parabolic ones in the fully-developed region. Comparison of the solid and dashed curves indicates that mass transfer has little effect on the developments of velocity profiles, except for the results at downstream region. At downstream region, the mass flow rate is large for the system with mass transfer due to the film evaporation along the wetted walls. A rise in wall temperature T_1 (see Fig. 2(a) and (b)) results in a higher axial velocity U, in conformity with the fact that a greater amount of water vapor evaporates into the flow for a higher T_1 and a larger buoyancy force through thermal diffusion. Change of radii ratio λ (see Fig. 2(a) and (c)) shows that a smaller λ gives a larger u/u_0. This can be made plausible by noting the fact that the system with a smaller λ

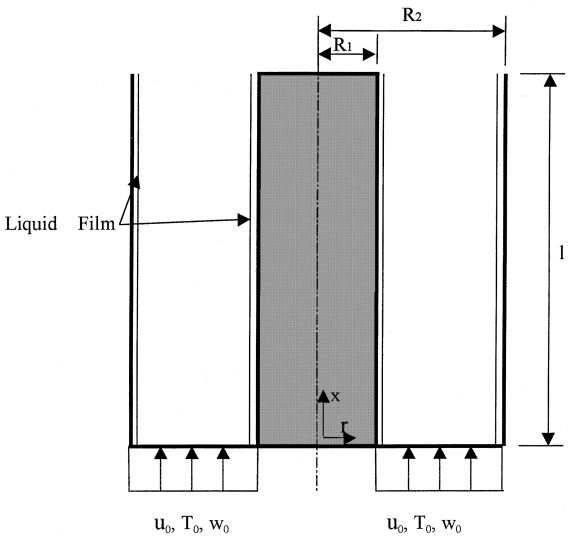

Fig. 1. Schematic diagram of the physical system.

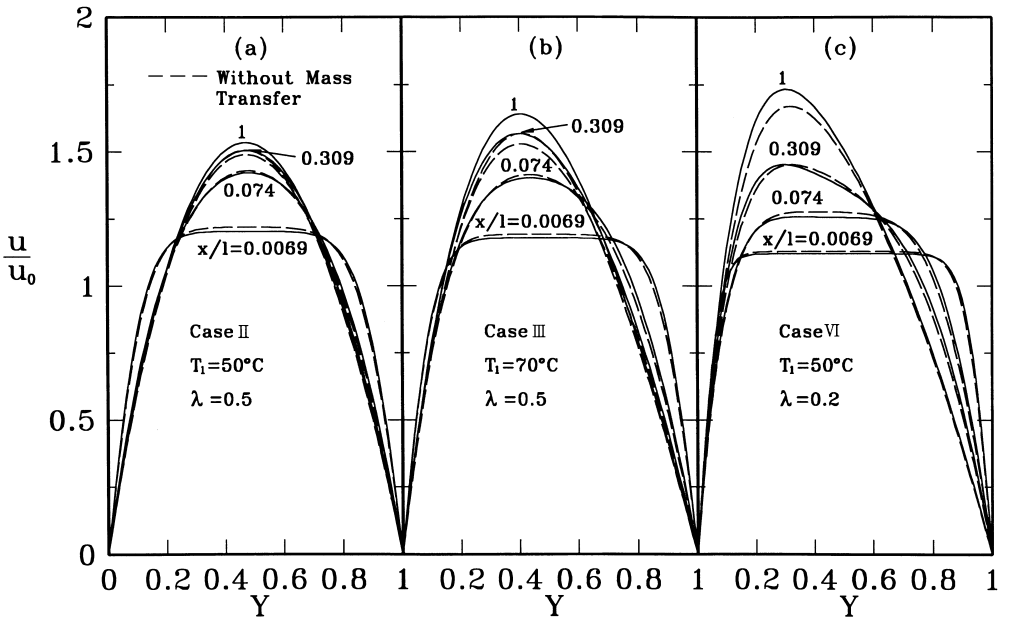

Fig. 2. The developments of axial velocity profiles.

gives larger combined buoyancy forces, i.e., larger Gr_T and Gr_M (by checking Table 1).

Shown in Figs. 3 and 4 are the axial developments of dimensionless temperature and mass-fraction profiles, respectively. Because the outer wetted wall is fixed at $T_2 = 30°C \leqslant T_1$, the saturated mass-fraction on the outer wall w_2 is thus smaller than that on the inner wall w_1. According to the definition of θ and W in Eq. (5), θ and W on the outer wetted wall are, therefore, less than unity. It is interesting to observe that the developments of temperature profiles are faster for the system without mass diffusion. This is due to the smaller buoyancy forces for the system without mass diffusion. By comparing Figs. 3 and 4, it is found that the profiles for θ

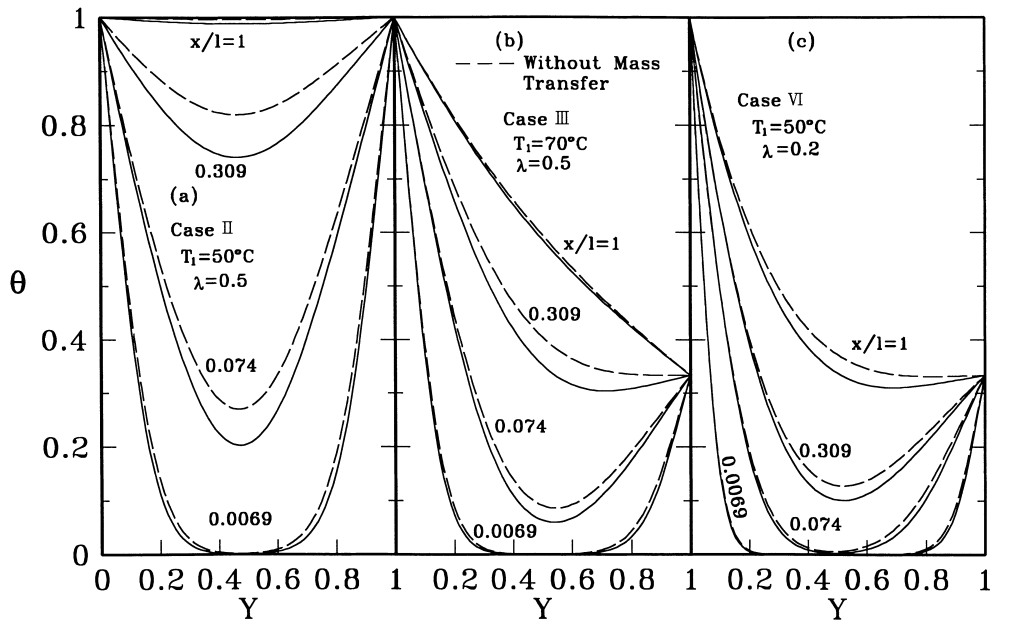

Fig. 3. The developments of axial temperature profiles.

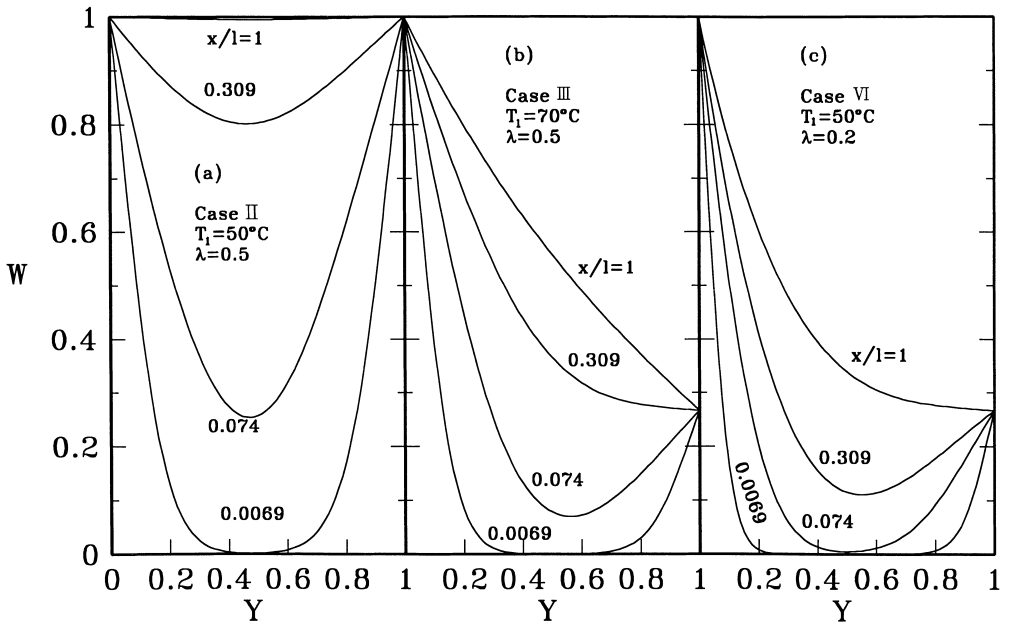

Fig. 4. The developments of axial concentration profiles.

and W develop in a rather similar fashion. Careful inspection, however, discloses that the mass-fraction boundary layers develop little more rapidly than the thermal boundary layers do. This simply results from the fact that Pr is slightly larger than Sc in the flow. Also to be seen in Fig. 4 is that, in the initial portion of the duct, the mass-fraction of water vapor in the flow is still small relative to those on the wetted walls. But as the moist air goes downstream, the mass-fraction of water vapor in the air stream gradually increases owing to the liquid film vaporization from the wetted walls. Thus the concentration level of water vapor near the outer wall could be higher than w_2 beyond a certain axial location. This is clearly seen in Figs. 4(b) and (c) or Fig. 6. This implies that the water vapor in the flow will condense on the outer wall after this location. Therefore, in the entry portion of the duct the liquid film on the outer wall vaporizes but condensation of water vapor in the moist air occurs in the downstream region.

The effects of the inner wetted wall temperature T_1 on the local heat and mass transfer along the inner wall are presented in Fig. 5. According to the definition of Nusselt numbers, Eq. (12), the latent heat Nusselt number Nu_{l1} equals to the difference of Nu_{x1} and Nu_{s1}. An overall inspection on Fig. 5 reveals that the heat transfer due to latent heat transport associated with the film evaporation is much more effective than that due to sensible heat transfer connected to the temperature difference. Moreover, a larger $Nu_l(Nu_{x1} - Nu_{s1})$ is noted for a system with a higher T_1. This is resulted from the stronger film evaporation at a higher wetted wall temperature. In Fig. 5(c), the variations of the local Sher-

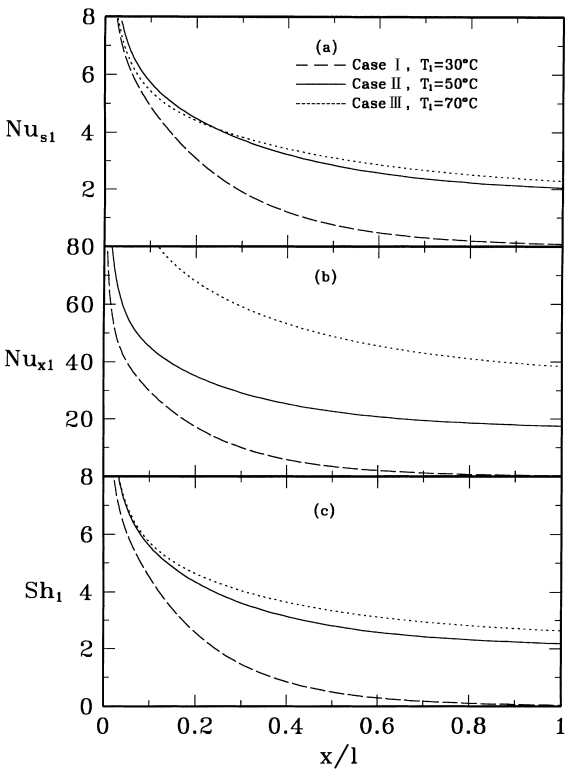

Fig. 5. Effects of inner wall temperature T_1 on the local Nusselt and Sherwood number distributions along the inner wetted wall: (a) sensible heat Nusselt number; (b) interfacial Nusselt number; (c) Sherwood number.

wood number Sh_1 are similar to those of sensible heat Nusselt number Nu_s. Smaller Nu_{s1} and Sh_1 are found for a system with a lower T_1 due to the smaller combined buoyancy effects.

Attention is turned to investigate the heat and mass transfer along the outer wetted wall whose temperature is maintained at $T_2 = 30$°C. Fig. 6 shows the effects of inner wall temperature T_1 on the local heat and mass transfer on the outer wall. Careful scrutiny of Fig. 6 indicates that in the initial portion of the channel the distributions of Nu_{s2}, Nu_{x2} and Sh_2 are positive. But as the moist air goes downstream, the values of Nu_{s2}, Nu_{x2}, and Sh_2 change sign and become negative for the cases with $T_1 = 50$ or 70°C. This implies that after some certain location, the water vapor in the moist flow would condense along the outerwall. Additionally, it is noted that the location at which Sh_2 changes sign is closer to the inlet for the system with a higher T_1. This is a direct consequence of a larger amount of water vapor evaporation from the inner wall.

The effects of the relative humidity of moist air at inlet on the local latent heat Nusselt number along the inner and outer walls are presented at Fig. 7. In line with

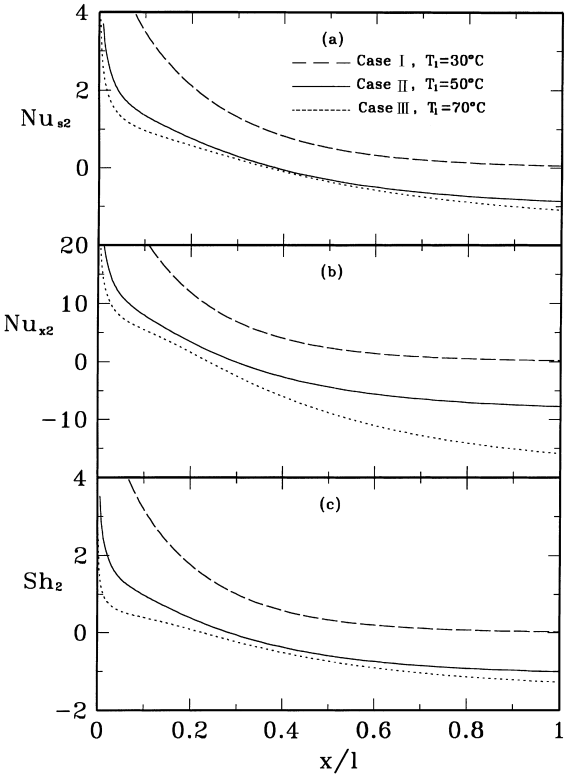

Fig. 6. Effects of inner wall temperature T_1 on the local Nusselt and Sherwood number distributions along the outer wetted wall: (a) sensible heat Nusselt number; (b) interfacial Nusselt number; (c) Sherwood number.

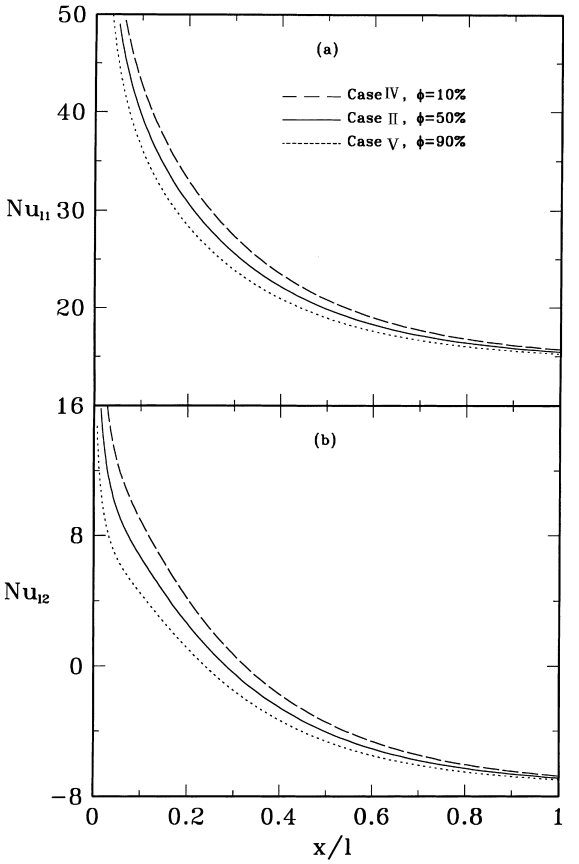

Fig. 7. Effects of relative humidity of moist air ϕ on the latent heat Nusselt numbers along the the wetted walls.

the common sense, a larger Nu_l is found for a system with a lower ϕ due to the larger driving potential of mass transfer between the moist air and wetted walls. In addition, it is observed in the separate numerical runs that the effects of ϕ on the distributions of velocity and temperature are relatively insignificant.

In the study of natural convection heat and mass transfer in vertical annuli, the knowledge of radii ratio $\lambda(= R_1/R_2)$ on the heat and mass transfer is important. Figs. 8 and 9 present the effects of radii ratio λ on the local Nusselt and Sherwood numbers along the inner and outer walls, respectively. It is clearly that larger Nu and Sh results for a system with a smaller λ due to a higher combined buoyancy effects. This can be checked by noting Table 1.

The flow rate driven into the vertical duct by the combined buoyancy forces is an important characteristic of the problem studied. This is investigated in Fig. 10, where the Reynolds number Re is based on the hydraulic diameter $D_h = 2(1-\lambda)R_2$ and inlet velocity u_0. For a given curve the duct length l is varied with other parameters (T_1, T_2, ϕ and λ) are fixed. In this plot, the l_r

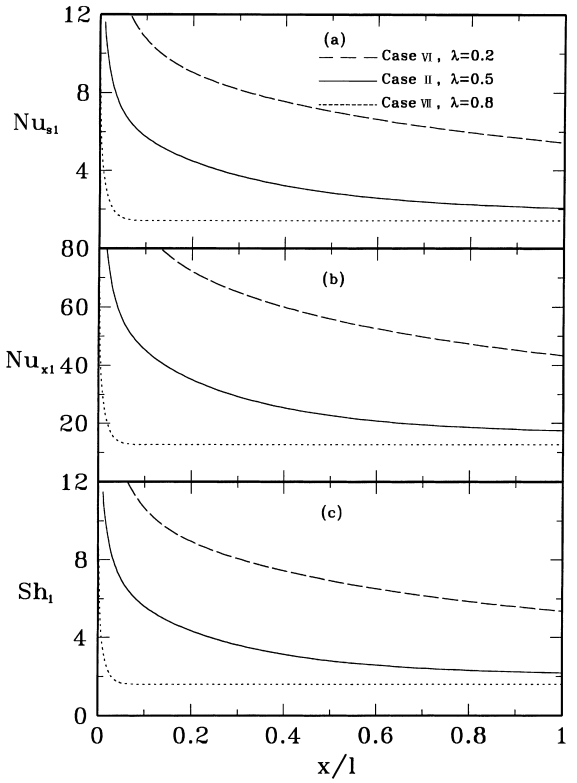

Fig. 8. Effects of radii ratio λ on the local Nusselt and Sherwood number distributions along the inner wetted wall: (a) sensible heat Nusselt number; (b) interfacial Nusselt number; (c) Sherwood number.

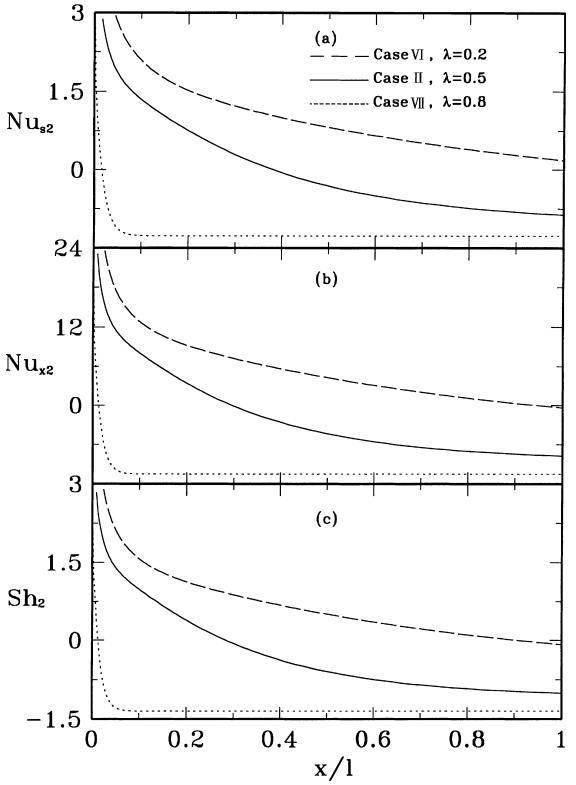

Fig. 9. Effects of radii ratio λ on the local Nusselt and Sherwood number distributions along the outer wetted wall: (a) sensible heat Nusselt number; (b) interfacial Nusselt number; (c) Sherwood number.

is the reference length and is chosen to be 1 m. It is clear that the induced Reynolds number *Re* increases significantly with an increase in channel length, especially for shorter channel. This is due to the chimney effect. But as the duct goes longer, the *Re* gradually increases. Additionally, a higher *Re* is noted for a system with a higher T_1 due to the larger buoyancy effects (by comparing cases I, II and III).

Finally, it is worthwhile to notice limits of applicability of the present flow model and hence of the results. For this purpose, recourse is necessary to the complete Navier–Stokes, energy and concentration equations, which describe more precisely the case under consideration. One can readily demonstrate that the present dimensionless governing equations of momentum, energy, and concentration have been obtained by omitting all powers of $R_2/l(Gr_{\mathrm{Tr}} + Gr_{\mathrm{Mr}})$ from the corresponding complete dimensionless equations. Therefore, such a simplification is permissible, and hence the present results are valid as long as the dimensionless group $R_2/l(Gr_{\mathrm{Tr}} + Gr_{\mathrm{Mr}})$ is much smaller than unity. Indeed, the condition of $R_2/l(Gr_{\mathrm{Tr}} + Gr_{\mathrm{Mr}})$ is always encountered in most practical situations.

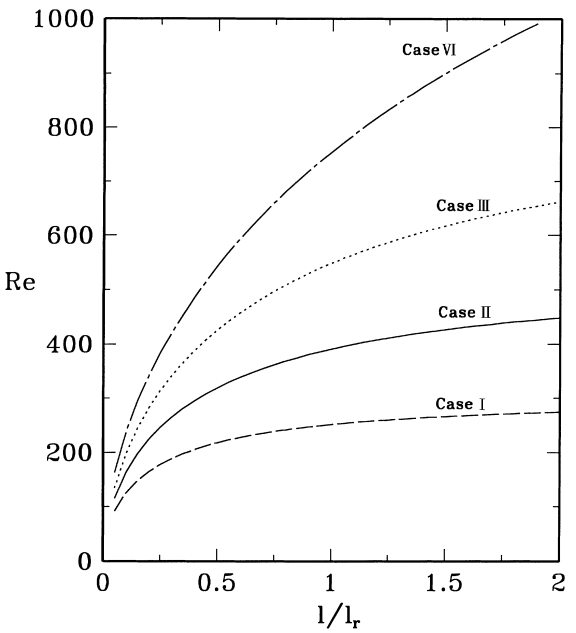

Fig. 10. Effects of duct length on the induced Reynolds number at inlet.

5. Conclusion

Laminar natural convection flows in vertical annulus ducts induced by the combined buoyancy effects of thermal and mass diffusion has been studied. The effects of the inner wetted wall temperature T_1, relative humidity of moist air at inlet ϕ, and radii ratio λ on the momentum, heat and mass transfer are examined in detail. What follows is brief summary of the major results.

1. Heat transfer along the wetted walls is dominated by the latent heat transport in association with water film evaporation or condensation. A larger Nu_1 results for a system having a higher T_1.
2. Due to a larger amount of water vapor evaporated into the air stream for the system with a higher T_1, the axial position, where the incipience of the condensation along the outer wall is closer to the channel inlet.
3. Better heat and mass transfer is noted for a system with a larger radii ratio λ due to the larger combined buoyancy effects.
4. The induced flow rate by the combined buoyancy forces of thermal and mass diffusion increases significantly with channel length l as the duct is short, while for the long channel the increase is gradual.

Acknowledgements

The author would like to acknowledge the financial support of the present work by the National Science Council, R.O.C., through the contract NSC87-2212-E211-006.

References

[1] M.A.I. El-Shaarawi, A. Shrhan, Developing laminar free convection in a heated vertical open-ended annulus, Ind. Eng. Chem. Fundam. 20 (1981) 388–394.
[2] M.A.I. El-Shaarawi, A. Shrhan, Developing laminar free convection in an open ended vertical annulus with a rotating inner cylinder, ASME J. Heat Transfer 103 (1981) 552–558.
[3] M. Al-Arabi, M.A.I. El-Shaarawi, M. Khamis, Natural convection in uniformly heated vertical annuli, Int. J. Heat Mass Transfer 30 (1987) 1381–1389.
[4] H.M. Joshi, Numerical solutions for developing laminar free convection in vertical annular ducts open at both ends, Numer. Heat Transfer 13 (1988) 393–403.
[5] D. Littlefield, P. Desai, Buoyant laminar convection in a vertical cylinder annulus, ASME J. Heat Transfer 108 (1986) 814–821.
[6] B. Gebhart, L. Pera, The nature of vertical natural convection flows resulting from the combined buoyancy effects of thermal and mass diffusion, Int. J. Heat Mass Transfer 14 (1971) 2025–2050.
[7] L. Pera, B. Gebhart, Natural convection flows adjacent to horizontal surfaces resulting from the combined buoyancy effects of thermal and mass diffusion, Int. J. Heat Mass Transfer 15 (1972) 269–278.
[8] T.S. Chen, C.F. Yuh, Combined heat and mass transfer in natural convection on inclined surfaces, Numer. Heat Transfer 2 (1979) 233–250.
[9] T.S. Chen, C.F. Yuh, Combined heat and mass transfer in natural convection along a vertical cylinder, Int. J. Heat Mass Transfer 23 (1980) 451–461.
[10] J. Srinivasan, D. Angirasa, Numerical study on double-diffusion free convection from a vertical surface, Int. J. Heat Mass Transfer 31 (1988) 2033–2038.
[11] T.S. Lee, P.G. Parikh, A. Acrivos, P. Bershader, Natural convection in a vertical channel with opposing buoyancy forces, Int. J. Heat Mass Transfer 25 (1982) 499–511.
[12] D.J. Nelson, B.D. Wood, Combined heat and mass transfer natural convection between vertical parallel plates with uniform flux boundary conditions, Heat and Mass Transfer 4 (1986) 1587–1592.
[13] D.J. Nelson, B.D. Wood, Combined heat and mass transfer natural convection between vertical parallel plates, Int. J. Heat Mass Transfer 32 (1989) 1779–1787.
[14] W.M. Yan, T.F. Lin, Combined heat and mass transfer in natural convection between vertical parallel plates with film evaporation, Int. J. Heat Mass Transfer 33 (1989) 529–541.
[15] C.J. Chang, T.F. Lin, W.M. Yan, Natural convection flows in a vertical open tube resulting from combined buoyancy effects of thermal and mass diffusion, Int. J. Heat Mass Transfer 29 (1986) 1543–1552.
[16] L.C. Chow, J.N. Chung, Evaporation of water into a laminar stream of air and superheated stream, Int. J. Heat Mass Transfer 26 (1983) 373–380.
[17] T. Fujii, Y. Kato, K. Mihara, Expressions of transport and thermodynamic properties of air, stream and water, Report No. 66, Department of Production Science, Kyu Shu University, Kyu Shu, Japan, 1977.
[18] R.B. Bird, W.E. Stewart, E.N. Lightfood, Transport Phenomena, Wiley, New York, 1960.
[19] E.R.G. Eckert, R.M. Frake Jr., Analysis of Heat and Mass Transfer, McGraw-Hill, New York, 1972.
[20] S.V. Patankar, Numerical Heat Transfer and Fluid Flow, Hemisphere/McGraw-Hill, New York, 1980.